A STUDY OF THE OPTICAL PROPERTIES OF QUANTUM WELL SOLAR CELLS AIMED AT OPTIMIZING THEIR CONFIGURATION

Paul STERIAN [1], Silvian FARA[2], Laurentiu FARA[3], Mihai IANCU[4]

Această lucrare este bazată pe contribuţii originale dezvoltate în cadrul proiectului CEEX ***Cercetări privind creşterea eficienţei celulelor fotovoltaice nanostructurate–NANO_PV (2006-2008)*** *[1] privind influienţa parametrilor optici ai celulelor solare cu gropi cuantice, asupra randamentului de conversie. A fost abordată modelarea optică şi simularea numerică pentru coeficientul de absorbţie, indicele de refracţie precum şi reflectanţa. Totodată a fost stabilită configuraţia optimă a celulelor cu gropi cuantice multiple (MQW).*

This paper is based on the original contributions developed within the CEEX project ***Research regarding the efficiency increasing of nanostructured photovoltaic cells –NANO_PV (2006-2008)*** *[1] regarding the influence of the optical parameters of the quantum well solar cells, upon conversion efficiency. It was considered optical modelling and simulation for absorption coefficient, refraction index, as well as upon reflectance. It was established the optimized configuration of the Multi – Quantum Wells (MQW).*

Key words: quantum well solar cells, optimization, quantum confining, multi-band structure, hybrid model.

1. Introduction

Quantum dot solar cells are based on the advantages of low-sized systems. There are two main contributions:

- **The first** is the powerful quantum confining (***QC***) effect, because at quantum dimensions, the nature of the material plays a secondary role.

- **The second** contribution is given by the increased role of the surfaces/interfaces. Indeed, the ratio between the number of atoms on the surface

[1] Professor, Faculty of Applied Sciences, Physics II Chair, University POLITEHNICA of Bucharest, Romania, e-mail:sterian@physics.pub.ro

[2] Researcher, IPA SA - Research development, engineering and manufacturing for automation equipment and systems**,** , Romania

[3] Professor, Faculty of Applied Sciences, Physics II Chair, University POLITEHNICA of Bucharest, Romania

[4] Researcher, IPA SA - Research development, engineering and manufacturing for automation equipment and systems , Romania

of a low-sized system (0D, 1D, 2D or fractal) and the total number of atoms is $N_S/N = 2(3-\delta)a/d$, where δ is system dimensionality, a is the inter-atomic distance (determining the thickness of the surface layer and depending on its orientation with respect to the crystalline axes), and d is the (minimum) dimension of the system [2], [3].

In multiple quantum wells (**Multi-Quantum Wells – MQW**) cells not only layer thickness is important, but also their regularity and mostly their number, due to reasons similar to those that define quantum dimensions. One can see that, besides the resonant levels/mini-bands of the conduction and valence bands of the layers with quantum wells, there are a number of levels in the energy gaps, both in the layers with quantum wells and in the barrier ones. These confining levels contribute tot extending the absorption spectrum (figure 1).

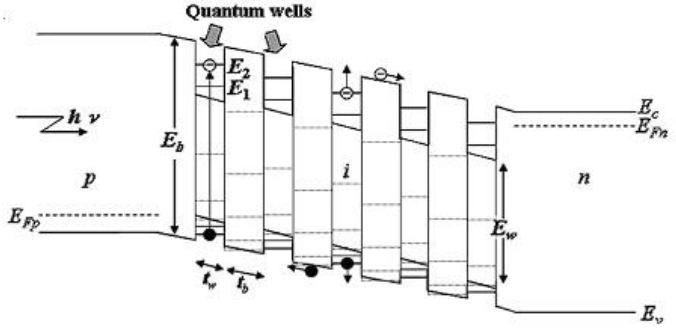

Fig. 1. p-i-n quantum solar cell: multilayer structure.

The present paper approaches optical modelling and simulation of some optical processes (absorption, reflection, refraction) aiming to establish the optimal configuration of MQW solar cells. The results of the study are in good agreement both with the experimental ones and with the simulated results obtained by other authors ([4, 5, 6, 7, 8]).

2. Optical modelling of quantum well solar cells

2.1 Absorption processes in multi-band solar cells

A. *Finite bandwidth*

A method to ensure the required selectivity of photons is to have finite but acceptably small widths for all the bands involved in the cell [9]. In the case of a cell with three bands, the optimal choice is to have a quite narrow mid-band, just like in the case of one impurity band (figure 2). This medium band is ideally separated from one of the other bands (for example, from the valence band), through 0.7eV, and from the other one (the conduction band respectively), through 1.2eV; hence the optimal interval between the lower and the upper band

is 1.9eV. Photons with energy between 1.9eV and 3.1eV can excite electrons from the valence band, up to the conduction band.

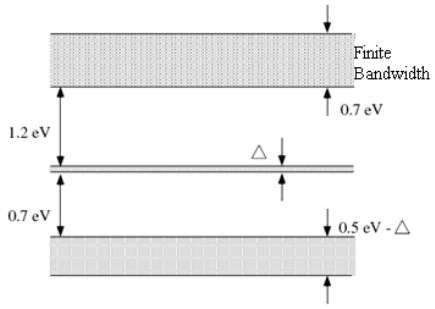

Fig. 2. Solar cell with 3 bands, optimally designed, with photon selectivity ensured by the finite width of each of the 3 bands involved

The disadvantage for this approach to photon selectivity is that there is a peak of the maximum energy of a participating photon (with the value of 3.1eV). This reduces *the quantum efficiency* that can be achieved for an optimized solar cell, from 63.2 % to 57, and 1 %. In practice, this result is not a severe limitation, due to adequate filtering of photons with high levels of energy (either naturally through the ozone layer or through UV filters) [10, 11].

B. *Graded absorption coefficients*

The second approach to ensure photon selectivity is to establish a gradation in the absorption properties, so that the processes with the largest energy will be highly absorbent, and those with the lowest energy will be the least absorbent. This ensures that the photons with high levels of energy will be preferentially absorbed in those processes that can put them into use. One remarked that the gradual usage of absorption coefficients in the range 10-100 leads to quantum efficiencies close tot the limit efficiency (63.2%) [11].

C. *Spatial distribution of absorption*

The third approach is based on the spatial distribution of absorption. The cell is designed in such a way that light is transmitted to a region in which the high energy photons can be filtered. Then, light passes through a zone in which high and medium energy photons can be absorbed, and finally reaches a layer capable to absorb low energy photons. Figure 3 presents three such situations. The spatial approach allows the optimal use of the light accepted by the cell, without ensuring a guarantee for recycled photons.

The approach in figure 3(a) uses an impurity band as an intermediary band. When the impurity band is missing, the photons with large energy are absorbed near the cell surface through band-band processes. Doping is used to control the grade of occupation of the impurity band, so that in the point in which light passes

through it for the first time, it is filled with electrons, being possible to excite these electrons in the conduction band. On the back of the device, doping is once again used to make sure that the impurity band is depleted of electrons, increasing the transitions from the valence band towards it.

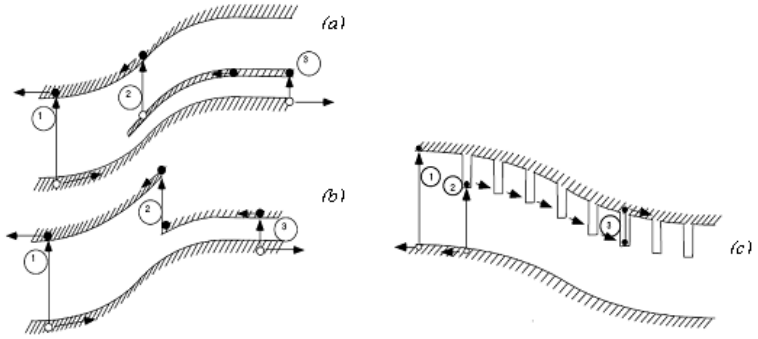

Fig. 3. Three approaches for the selective absorption of photons: **(a)** impurity band; **(b)** hetero-junction interface; (c) multiple quantum wells

In fig. 3(b) one uses the interface between a wide *gap* and a narrow one in the semiconductor, and hence the carriers could be optically excited through the interface. But, this light absorption process is relatively low, as compared to the other two processes of spatial distribution of absorption. Figure 3(c) presents a schema of selective absorption based on multiple quantum wells. Absorption is controlled spatially through doping the host semiconductor. For a cell with three bands to work, the jump of the carriers between different states for neighbouring quantum wells has to be more efficient than getting out of the well [12].

D. *Modelling of absorption coefficient*

In applications with computing of solar cell efficiencies, the absorption coefficient is described by continuous functions. For GaAs, fitting the experimental data one determined the following function that approximates *the absorption coefficient*:

$$\alpha_{\mathrm{GaAs}}(\lambda)=\begin{cases} \mathrm{e}^{y_1(\lambda)}, & 0.7<\lambda\le 0.88\ \mu\mathrm{m} \\ \mathrm{e}^{y_2(\lambda)}, & 0.24<\lambda\le 0.7\ \mu\mathrm{m} \\ \mathrm{e}^{y_2(0.24)}, & 0<\lambda\le 0.24\ \mu\mathrm{m} \\ 0, & \text{otherwise} \end{cases} \tag{1}$$

$$y_1(\lambda)=-0.7863+5.3115\left[1+\mathrm{erf}\left(-\frac{\lambda-0.84291}{0.038}\right)\right] \tag{2a}$$

$$y_2(\lambda)=-447.432+4201.2\lambda^2+6835.128\lambda^2\ln\lambda-3781.193\lambda^3+\frac{3.9049}{\lambda^2} \tag{2b}$$

(a) 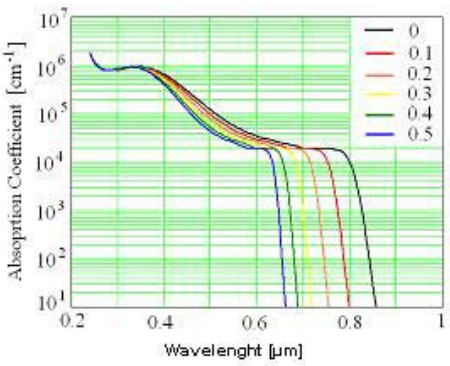

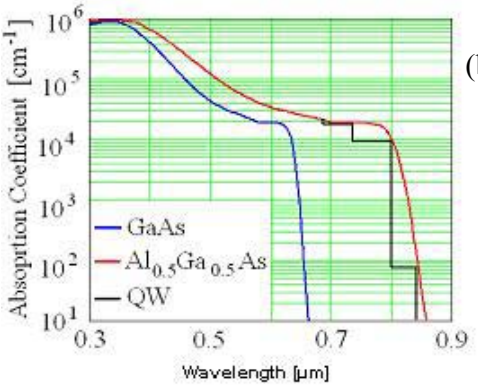

(b)

Fig. 4. **a).** The absorption coefficient for $Al_xGa_{1-x}As$ vs. the wavelength (x is the curve parameter). **b).** Absorption coefficient in GaAs crystal, in the ternary composite $Al_{0.5}Ga_{0.5}As$ computed through the translation of axis method, and in the MQW system.

Fig. 4a shows the diagram of the absorption coefficient for GaAs computed with the algorithm for different alloy compositions. Fig. 4b compares the absorption coefficients in GaAs, $Al_{0.5}Ga_{0.5}As$ and in the MQW system. Hence once energy increases the absorption coefficient in the MQW system increases step-by-step, due to the quantization of the density of states on the confining direction of the carriers [1].

2.2 Modelling of the refraction index and of the reflectance of multiple quantum well solar cells

A. *Modelling and simulation of refraction index*

Determination of the refraction index of semiconductor materials can be done with the Kramers-Krönig relations. By combining the refraction index model with the Fresnel relations, one can evaluate the losses through reflection in the quantum well solar cells [13].

The refraction index can be introduced by means of the complex electric permittivity of a dielectric material:

$$\varepsilon(\omega) = \varepsilon_1(\omega) + i\varepsilon_2(\omega) \tag{3}$$

where $\varepsilon_1(\omega) = n^2$ (n being the refraction index), and $\varepsilon_2(\omega)$ is associated to the coefficient of absorption.

After a series of successive refinements operated by means of the ***MSEO*** (*Modified Single Effective Oscillator*) model, one obtains [14]:

$$n^2 = 1 + \frac{E_d}{E_o} + \frac{E_d}{E_o^3}E^2 + \frac{\eta}{\pi}E^4 \, ln\left(\frac{2E_o^2 - E_g^2 - E^2}{E_\Gamma^2 - E^2}\right) \tag{4}$$

where $E = \hbar\omega$ is photon energy (eV).

The other parameters in relation (2) were obtained experimentally [15], leading to *the oscillator energy*:

$$E_o = A + BE_\Gamma \tag{5}$$

where E_Γ is the lowest direct *gap* (and $A \sim 2.6$, $B \sim 0.75$),

The dispersion energy is: $$E_d = \frac{F}{E_0} \tag{6}$$

F is correlated by the (simplified) Kramers–Krönig relation and

$$F = \omega_p{}^2 f_n \tag{7}$$

where ω_p represents the plasma frequency and f_n is the oscillator strength, calculated by Harrison [16].

Based on the results obtained by Barnham [3], one should mention that the quantum wells in these solar cells have the role of using the spectrum region that is usually not adequate for producing a pair of photon carriers in the conduction and in the valence band, but can generate particles in the respective quantum wells. One uses the following expression for *the refraction index* of (4) relation, parameters E_g, E_Γ, E_o and E_d are given by: $E_g = 1.6729eV$; $E_\Gamma=1.4235eV$; $E_o=2.6+0.75E_\Gamma$; $E_d= F/E_o$. Parameter η is given by the expression:

$$\eta = \frac{\pi E_d}{2E_o^3\left(E_o^2 - E_\Gamma^2\right)} \tag{8}$$

The results of simulating the refraction index vs. the photon energy (simplified model) are illustrated in figure 5.

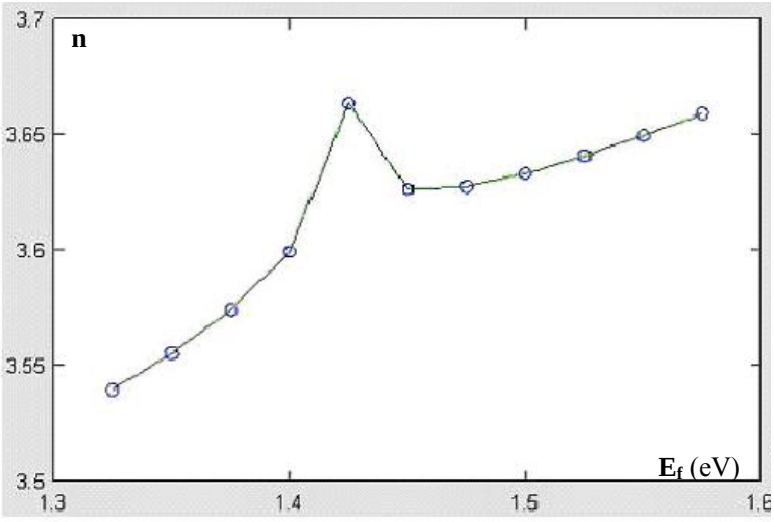

Fig. 5. The refraction index of the quantum well solar cells vs. photon energy

Rault [17] improved the refraction index model developed by Chih-Hsiang Lin & co. in 1994 [18], the results of simulation being presented in figure 6. The

device used for comparison is a quantum wells modulator. This is due to the lack of data directly connected to the refraction index of quantum well solar cells.

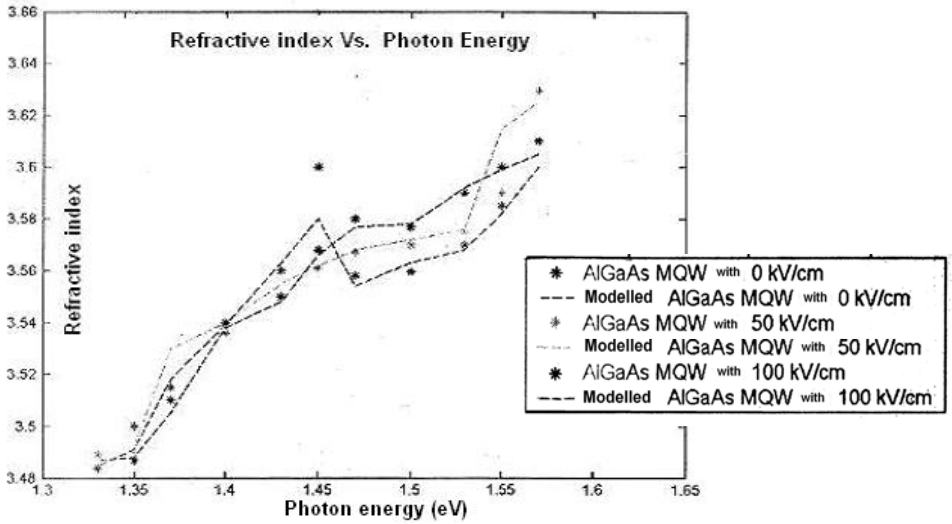

Fig.6. The index of refraction of quantum well solar cells; comparison between the results of the Rault and Chih-Hsiang Lin models for cells with AlGaAs, in electric fields of 0-100kV/cm

For simulation, one considered the following solar cell structure: AlGaAs/GaAs (x = 0.2) with 25 quantum wells, each 10nm in length, and the potential barrier also being 10nm in length. The dashed lines, represent the results generated by the Rault model, and the ones marked with asterisk (*) are generated by the Chih-Hsiang Lin model. The Rault model delivers values very similar with those of the Chih-Hsiang Lin model, with a ~ 0.3% error for the relative energy levels.

In the Rault model of the index of refraction, when the electric field increases, the excitation energy is significantly reduced, reaching zero for an electric field of 100kV/cm. Presence of the excitation effects is attributed to the absorption coefficient of the quantum wells. Because one wishes to use quantum wells to absorb the wavelengths under the *gap* of the semiconductor material, an electric field applied over the intrinsic region would determine a decrease in the presence of excitons, and hence in the absorption of the quantum wells.

The increase in Auger recombination determines an increase in the activity of the photons in the semiconductor material, leading to the generation of additional heat in the material and to a decrease in the conversion efficiency of the solar cell. Hence a doping level under $N \le 10^{15} / cm^3$ is recommended. When considering the effects of the excitonic energy on the energy levels in the quantum wells, one sees that its presence determines the transition energy levels to require more energy for the particle to escape the quantum well confinement. This

additional energy shall be obtained through thermal excitation, tunnelling or assisted photon migration. Because the energy levels are inversely proportional with the length of the quantum well, one can conclude that photo-carriers in the narrow quantum wells ($\leq 10nm$) would need less energy to leave the quantum well. This is based on the fact that the energy levels in a large quantum well will be lower towards the bottom of the quantum well, hence needing more energy to pass the barrier.

B. *Optimization of the reflectance of quantum well solar cells*

One can use the *refraction index* model to explore the relation between the *refraction index* and *reflectance*. To do this, the refraction index model has to be combined with the Fresnel relations, allowing determining the losses through reflection of the quantum wells structure. Solar cell reflectance ***R*** can be computed by using a Fresnel relation [19, 20]:

$$R = \frac{r_1^2 + r_2^2 + 2r_1 r_2 \cos 2\theta}{1 + r_1^2 r_2^2 + 2r_1 r_2 \cos 2\theta} \tag{9}$$

where: $r_1 = \frac{n_0 - n_1}{n_0 + n_1}$ $r_2 = \frac{n_1 - n_2}{n_1 + n_2}$ $\theta = \frac{2\pi n_1 d_1}{\lambda}$ (10)

The following notations were introduced: n_0 - refraction index of the incident medium; $n_0 = 1$ in the case of air; n_1 - refraction index of the anti-reflection layer; n_2 - refraction index of the substrate (quantum wells solar cell). Thickness d_1 of the anti-reflection layer can be determined by minimizing relation (10). It was shown that it is around 600-650nm, in the case of minimum reflection.

One can evaluate the effect of the number of quantum wells upon the refraction index, as well as upon the losses in reflection. Hence one can determine the optimum number of quantum wells in the structure [11].

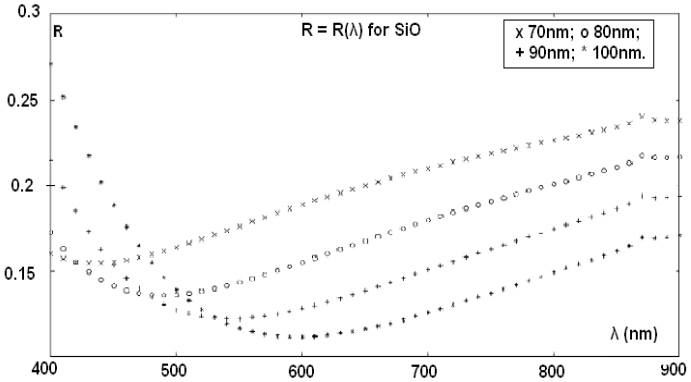

Fig. 7. Reflectance model for a solar cell with QWSC structure with a SiO anti-reflection layer

Figure 7 illustrates the results of the optical simulation of quantum well solar cells (based on equations (9) – (10) and on the model analysed for the refraction index through equations (7) and (8)), in the form of the dependency of reflectance (***R***) on the wavelength for different thicknesses (*d*) of the anti-reflection layer; one considered two types of anti-reflection layers ($n_1 = 1.4 - SiO$). The results generated by the model agree with the experimental ones [1].

The reflectance model can be used to determine the effects of varying the number of quantum wells, upon the refraction index.

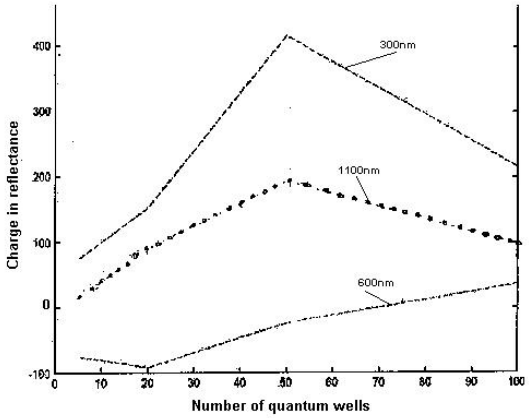

Fig. 8: Reflectance change (%) vs. the number of quantum wells of the solar cell.

Figure 8 presents the percentage change in reflectance for each quantum well structure, in comparison to the reference cell. It is evident that, for a certain wavelength, the change in reflectance induced by the change in the refraction index, through the variation of the number of quantum wells, is unique for that wavelength and can be significant (from 92% to 400%). Table 1 presents the results regarding the change in reflectance in the case of four structures, with 5, 20, 50 and 100 quantum wells.

Table 1

Percentage reflectance value depending on the number of quantum wells

Wavelength (nm)	5 quantum wells	20 quantum wells	50 quantum wells	100 quantum wells
300	73.39	15.44	415.45	215.61
600	-74.81	-92.07	-24.87	35.86
1100	5.54	92.37	193.38	72.81

In the case of the 1100nm wavelength, one remarks significant changes in reflectance at structures with 20 and 50 quantum wells, in comparison to the control structure. This suggests minimum losses due to reflectance along the

whole spectrum can be achieved with cell structures having between 20 and 50 quantum wells.

3. Optimization of the parameters of MQW solar cells

The MQW cell is a system containing both the *Quantum level* in which one computes the energy spectrum of the electron and the absorption coefficient of the MQW, and the *Macroscopic level* in which one studies the transport of charge carriers [21]. This mix of quantum and classical elements in modelling of the MQW solar cell gives the denomination of the *hybrid model* (***HM***).

Hereby is an exemplification of the HM model capability to evaluate the performances of the MQW cell. Figure 9 synthesises the results of computing the conversion efficiency for a cell with the following parameters $N_w = 30$, $l_w = 20$nm and $l_b = 10$nm. The ***I-V*** characteristic together with the power dissipated by the cell on the external circuit, are illustrated in figure 10a. Hence, the main parameters of the cell are obtained: $J_{SC} = 48.5$ mA/cm^2, $V_{CD} = 0.886$V, $F_f = 0.86$ and $\eta = 0.371$. The numerical values are close to the ones reported in literature. As long as for a conventional cell with p-n junction, the maximum possible efficiency is estimated to be around 34% [22], the result neither confirms nor invalidates the fact that the MQW insertion in improves the conversion efficiency.

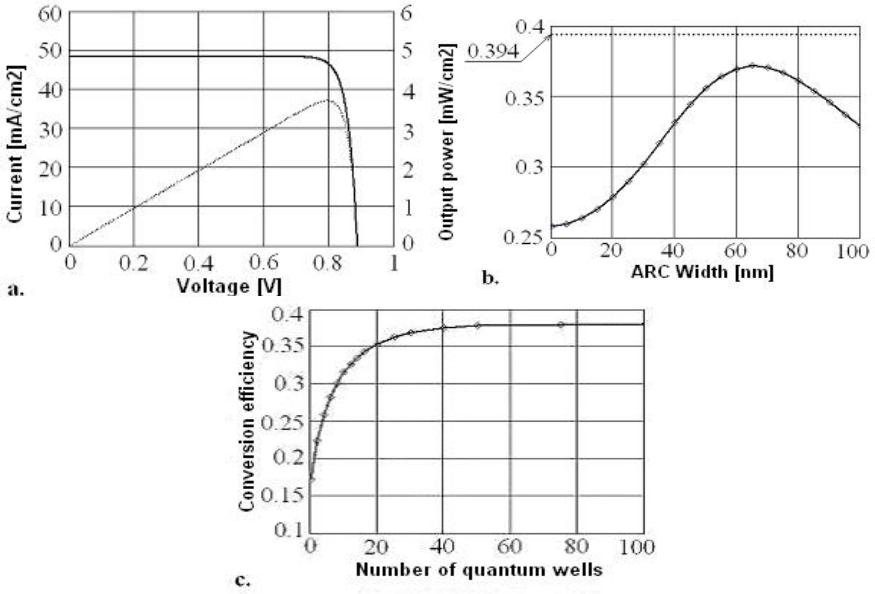

Fig. 9. **(a)** I-V characteristic (line) and the output power (points) of the MQW cell composed of: GaAs/$Al_{0.3}Ga_{0.7}As$, $N_w = 30$, $l_w = 20$nm, $l_b = 10$nm and a depth of the anti-reflection layer d = 64nm. **(b)** MQW cell efficiency vs. the depth of the anti-reflection layer. The dashed line illustrates the ideal cell efficiency, with zero reflectance.
(c) MQW cell conversion efficiency vs. the number of quantum wells.

Figure 9b shows the dependency of *the conversion efficiency* on *the depth of the anti-reflection layer*. One can see that in the ideal case, when the cell reflectance is neglected, the efficiency of the MQW cell based on $GaAs/Al_xGa_{1-x}As$ does not exceed 40%. In contrast to reflectance, in figure 9c one can see that conversion efficiency is strongly correlated to the number of quantum wells up to $N_w = 30$; Over this value, efficiency is saturated with respect to N_w. This is due to the path that light travels inside the MQW system; saturation appears when the length of the path travelled by light is comparable to the length of absorption.

This is a first approach of using the HM model for optimization of the parameters of MQW solar cells. Knowing the materials in the composition of the MQW cell [16] and their optoelectronic properties, for a given geometric configuration one can determine the parameters of the cell, particularly the conversion efficiency. Of course the computation can be repeated by varying the different geometrical or material parameters in order to determine the optimum configuration, i.e. the one that maximizes efficiency.

4. Conclusions

The main results obtained during simulation are:

- One can evaluate the effect of the number of quantum wells upon the refraction index, as well as upon the losses through reflection. Hence one can determine the optimum number of quantum wells in the structure;
- The reflectance model can be used to determine the effects of variations in the number of quantum wells upon the refraction index;
- The simulated results are agreed with the experimental ones.

Acknowledgement

We'd like to acknowledge and thank our collaborators in the University Politehnica of Bucharest, in the West University of Timisoara and in the University Politehnica of Timisoara for the good and fruitful collaboration in developing the NANO-PV CEEX project.

R E F E R E N C E S

[1] Final Technical Report "*Research concerning increase in the efficiency of nanostructured solar cells" - NANO_PV Project* (in Romanian), Research contract no: 247/2006 - 2008
[2] *K. W. J. Barnham and G. Duggan,* J. Appl. Phys., 67, 3490, 1990.
[3] *K. W. J. Barnham, B. Braun, J. Nelson, M. Paxman*, Appl. Phys. Lett., 59, 135, 1991
[4] *K. W. J. Barnham,* A novel approach to higher efficiency - the quantum well solar cell, 11th E. C. Photovoltaic Solar Energy Conference, Montreux, Switzerland, pp. 146-149, 1992.

[5] *L. Fara, V. Iancu, M.R. Mitroi, E. Nistor, "*Physics bases of nanotechnology. Applications and perspectives" (in Romanian), *Punct* Publ. House, Bucharest, 2007.
[6] *M. Paulescu E. Tulcan-Paulescu, A. Neculae P. Gravila,* Internal Reflection Influence on the Multiple Quantum Well Solar Cell Efficiency JOAM, Vol. 10 (9): 2441-2444, 2008.
[7] *L. Cuadra, A. Marti, A. Luque,* Modelling of the absorption coefficient of the intermediate band solar cell, Proceedings of the 16th European Photovoltaic Solar Energy Conference, Glasgow, May, 15-21, 2000.
[8] *V. Ninulescu, V. Nicolae, A. Sterian,* Quantum–well lasers for medical industry, **(***Editor* Elloumi, M.. et al.), Bioinformatics Research and Development – BIRD 2008, CCIS13, pp. 563-570, Publ. House Springer, 2008
[9] *M.A. Green,* Journal Material Science B, pp. 65-71, 2000.
[10] *V. Iancu, M.R. Mitroi, L. Fara,* Modelling of multi-layered quantum well photovoltaic cells U.P.B. Scientific Bulletin, Series A, Vol. 71, Iss. 4, pp.53-63, 2009
[11] *L. Fara, M.R. Mitroi, V. Iancu, G. Milescu, G. Noaje,* Modelling and numerical simulation of nanostructured Solar Cells (in Romanian), Volume 2, *Punct* Publ. House, Bucharest, 2008
[12] *F. Capasso, et al.,* Appl. Phys. Lett., 47: 420, 1985
[13] *R. Rogojan; P.E. Sterian; A.R. Sterian; M. Elisa,* Spectral behaviour and nonlinear optical properties of aluminophosphate semiconductor - Doped glasses**,** Editor(s**):** P.A. Atanasov; S. Cartaleva, 11th International School on Quantum Electronics: Laser Physics and Applications, 4397358-361, 2001
[14] *I. Suemune,* INSPEC Publ. EMIS, 15, 283-287, 1996.
[15] *S. H. Wemple,* Phys. Rev. B., 7(8), 3767-3777, 1973.
[16] *P. Harrison,* Quantum Wells, Wires and Dots: Theoretical and Computational Physics, pp. 293, 180, Wiley, UK, 2000.
[17] *F. K. Rault,* Mathematical modelling of the refractive index and reflectivity of the quantum well solar cell, in Nanostructured materials for solar energy conversion (editor Soga, T.), Elsevier, Amsterdam, 2006.
[18] *Lin Chih-Hsiang, J.M. Meese, M.L. Wroge, Chun-Jen Weng*, IEEE PTL, 6(5), 623-625, 1994.
[19] *C. Rosu; D. Manaila-Maximean; D. Donescu, A. R. Sterian, et al.,* Influence of polarizing electric fields on the electrical and optical properties of polymer-clay composite system, Modern Physics Letters B**,** Volume: 24, Issue: 1, pp. 65-73, 2010
[20] *A. Goetzberger, J. Knobloch, B. Voss,* Crystalline Silicon Solar Cells, Wiley, London, pp. 14-19, 1998.
[21] *M. Graetzel,* Perspectives for dye-sensitized nanocrystalline solar cells, Progress in Photovoltaics, 8: 171-186, 2000
[22] *M. Paulescu, A. Neculae, E. Tulcan-Paulescu, D. Comanescu,* Numerical modelling of the nanostructured photovoltaic cells (in Romanian), Publ. House West University of Timisoara, 2008.